Published in final edited form as:

Aging Cell. 2008 December ; 7(6): 866–878. doi:10.1111/j.1474-9726.2008.00432.x.

Reduction of mitochondrial H_2O_2 by overexpressing peroxiredoxin 3 improves glucose tolerance in mice

Liuji Chen[1,2], **Ren Na**[2], **Mingjun Gu**[1,2], **Adam B. Salmon**[2], **Yuhong Liu**[1,2], **Hanyu Liang**[1,2], **Wenbo Qi**[1,2], **Holly Van Remmen**[1,2,3], **Arlan Richardson**[1,2,3], and **Qitao Ran**[1,2,3,¶]

[1]Department of Cellular and Structural Biology, University of Texas Health Science Center at San Antonio, Texas 78229

[2]Barshop Institute for Longevity and Aging Studies, University of Texas Health Science Center at San Antonio, Texas 78229

[3]South Texas Veterans Health Care System, San Antonio, Texas 78229

Summary

H_2O_2 is a major reactive oxygen species produced by mitochondria that is implicated to be important in aging and pathogenesis of diseases such as diabetes; however, the cellular and physiological roles of mitochondrial H_2O_2 remain poorly understood. Peroxiredoxin 3 (Prdx3/Prx3) is a thioredoxin peroxidase localized in mitochondria. To understand the cellular and physiological roles of mitochondrial H_2O_2 in aging and pathogenesis of age-associated diseases, we generated transgenic mice overexpressing Prdx3 (Tg(PRDX3) mice). Tg(PRDX3) mice overexpress Prdx3 in a broad range of tissues, and the Prdx3 expression is localized exclusively in the mitochondria. As a result of increased Prdx3 expression, mitochondria from Tg(PRDX3) mice produce significantly reduced amount of H_2O_2, and cells from Tg(PRDX3) mice have increased resistance to stress-induced cell death and apoptosis. Interestingly, Tg(PRDX3) mice show improved glucose homeostasis, as evidenced by their reduced levels of blood glucose and increased glucose clearance. Tg(PRDX3) mice are also protected against hyperglycemia and glucose intolerance induced by high-fat diet feeding. Our results further show that the inhibition of GSK3 may play a role in mediating the improved glucose tolerance phenotype in Tg(PRDX3) mice. Thus, our results indicate that reduction of mitochondrial H_2O_2 by overexpressing Prdx3 improves glucose tolerance.

Keywords

mitochondria; reactive oxygen species; aging; diabetes; oxidative stress; peroxiredoxin 3

Introduction

Mitochondria dysfunction is believed to underlie age-associated function losses and to contribute to pathogenesis of diseases such as diabetes and neurodegeneration (Ames et al.,

¶Corresponding author contact: Qitao Ran, Ph.D., University of Texas Health Science Center at San Antonio, Texas Research Park Campus, 15355 Lambda Drive, San Antonio, TX 78245-3207, ran@uthscsa.edu, Phone: 210-562-6129, FAX: 210-562-6130.

1995; Lowell and Shulman, 2005). Mitochondria are the major source of cellular reactive oxygen species (ROS), and ROS from mitochondria are believed to mediate the detrimental effects of mitochondria dysfunction (Harman, 1987; Nishikawa and Araki, 2007). $O_2^{\bullet -}$ and H_2O_2 are the two major species of ROS produced by mitochondria. Both $O_2^{\bullet -}$ and H_2O_2 are able to induce oxidative damage and thus are thought to play important roles in the development and progression of diseases such as diabetes and aging (Green et al., 2004). H_2O_2 produced by mitochondria participates in redox signaling though reversible oxidation of cysteine residues in target proteins; thus H_2O_2 is an important molecule for cell growth, differentiation and death (Rhee, 2006; Stone and Yang, 2006).

As part of the antioxidant system, the cell has evolved efficient means of reducing reactive oxidative species, and within the mitochondrion, H_2O_2 is mainly reduced by glutathione peroxidases and peroxiredoxins. Glutathione peroxidases in mitochondria include Gpx1 and Gpx4. However, Gpx1 is found both in cytoplasm and mitochondria (Panfili et al., 1991; Esworthy et al., 1997; Ho et al., 1997), while Gpx4 is localized in mitochondria, cytoplasm and various membrane factions and its primary role is to reduce lipid hydroperoxide in membrane (Brigelius-Flohe, 1999; Ran et al., 2004). Because of their high affinity toward H_2O_2, peroxiredoxins are efficient in removing low levels of H_2O_2 (Chae et al., 1999; Rhee et al., 2005). Peroxiredoxin 3 (Prdx3/Prx3) is a peroxiredoxin localized exclusively in the matrix of mitochondria (Cao et al., 2007; Zhang et al., 2007). Previous studies show that overexpression of Prdx3 in cell lines leads to reduced cellular ROS and that knockdown of Prdx3 in cells results in elevated cellular ROS (Chang et al., 2004; Matsushima et al., 2006; Hattori et al., 2003), suggesting that Prdx3 plays an important role in quenching H_2O_2 in mitochondria. Deficiency in Prdx3 is associated with Fanconi anemia (Mukhopadhyay et al., 2006) and neurodegenerative diseases such as amyotrophic lateral sclerosis (ALS), Parkinson's disease and Down syndrome (Wood-Allum et al., 2006; Krapfenbauer et al., 2003), suggesting that Prdx3 is an important protein in protecting an organism from pathogenesis of diseases.

Recent reports have suggested that reduction of mitochondria H_2O_2 by overexpression of catalase in mitochondria through genetic engineering may lead to retarded aging and prevention of diseases (Schriner et al., 2005; Anderson et al., 2008). Mitochondria ROS are also implicated to be important in development of diabetes (Green et al., 2004), and manipulations to reduce mitochondria ROS are shown to improve glucose tolerance and insulin sensitivity (Houstis et al., 2006). However, transgenic mice overexpressing Gpx1 develop insulin resistance and obesity (McClung et al., 2004). Because Gpx1 can reduce H_2O_2 at both cytoplasm and mitochondria, the specific effect of mitochondria H_2O_2 in regulating glucose tolerance remains controversial.

Although transgenic animal models with reduced mitochondrial production of H_2O_2 have been generated by targeting catalase into mitochondria (Schriner et al., 2005), no transgenic mouse models with reduced mitochondria H_2O_2 by overexpressing a native mitochondrial peroxidase are currently available. To further understand the cellular and physiological roles of mitochondrial H_2O_2 and to define the effects of reducing mitochondria H_2O_2 on aging and pathogenesis of age-associated diseases, we generated a transgenic mouse model overexpressing Prdx3: Tg(PRDX3) mice. Tg(PRDX3) mice overexpress Prdx3 protein

exclusively within mitochondria. As a result of increased Prdx3, mitochondria from Tg(PRDX3) mice produce significantly reduced amount of H_2O_2. Our results show that cells from Tg(PRDX3) mice have increased resistance to stress-induced cell death and apoptosis. Interestingly, Tg(PRDX3) mice show improved glucose homeostasis, as evidenced by their reduced blood glucose level and increased glucose clearance. In addition, Tg(PRDX3) mice are protected against hyperglycemia and glucose intolerance induced by high-fat diet feeding. We further show that the increased glucose homeostasis in Tg(PRDX3) mice is correlated with activation of Akt and inhibition of GSK3 in their liver tissues.

Results

Generation of Tg(PRDX3) mice

Transgenic mice were generated using a human BAC clone fragment containing the intact human PRDX3 gene plus approximately 16.5 kb and 6.7 kb of 5′- and 3′-flanking sequences, respectively. Line 1 of PRDX3 transgenic mice [Tg(PRDX3)] was used in this study; in this line of Tg(PRDX3) mice, Prdx3 mRNA levels (human PRDX3 mRNA from the transgene plus endogenous mouse Prdx3 mRNA) were increased by 3- to 5-fold in cerebral cortex, heart, liver, kidney, skeletal muscle and lung of the Tg(PRDX3) mice (Figure 1A). Tg(PRDX3) mice also have more total Prdx3 protein in all tissues than Wt mice, as indicated by the Western blot results in Figure 1B.

Increased Prdx3 in mitochondria from Tg(PRDX3) mice

To determine whether the high level of expressed Prdx3 in Tg(PRDX3) mice localizes to the mitochondria, we compared the levels of Prdx3 protein in cytosolic and mitochondrial subcellular fractions from the livers of Tg(PRDX3) and Wt mice. As previously reported (Chae et al., 1999), Prdx3 protein was localized only in mitochondria in Wt mice. More importantly, livers from Tg(PRDX3) mice showed a higher level of Prdx3 protein than Wt mice in the mitochondria fraction, but there was no expression of Prdx3 in cytosolic faction (Figure 1C), indicating that the Prdx3 protein expressed from the human PRDX3 transgene was localized only in mitochondria. We confirmed that Prdx3 in Tg(PRDX3) mice was localized exclusively to mitochondria using confocal laser microscopy (Figure 1D). Skin fibroblasts from Tg(PRDX3) mice have a 3.8-fold increase in Prdx3 mRNA compared to fibroblasts from Wt mice (data not shown), an increase that is similar to the levels of increase observed in various tissues from Tg(PRDX3) mice (Figure 1B). We first loaded fibroblasts with MitoTracker red to label mitochondria. After fixation, the cells were sequentially stained with anti-Prdx3 antibody and with an Alexa488-labeled secondary antibody. In the confocal laser scanning microscopy images (Figure 1D), the Prdx3 protein staining was shown in green whereas the mitochondria was shown in red. The merged picture of Prdx3 staining and mitochondria revealed a near perfect co-localization for Prdx3 protein and mitochondria (Figure 1D), indicating that the expressed Prdx3 protein resides exclusively within mitochondria in fibroblasts from Tg(PRDX3) mice.

Reduced production of H_2O_2 by mitochondria from Tg(PRDX3) mice

To determine whether overexpression of Prdx3 had an effect on mitochondrial H_2O_2 production, we isolated mitochondria from brain and skeletal muscle tissues of Tg(PRDX3)

mice and Wt mice that were 2–3 months of age. The level of mitochondrial H_2O_2 was measured using an amplex red-horseradish peroxidase method (Zhou et al., 1997; Muller et al., 2007). As shown in Figure 2A and 2B, compared to mitochondria from Wt mice, mitochondria from brain and skeletal muscle of Tg(PRDX3) mice had reduced H_2O_2 release in state 1. In the presence of glutamate/malate or in the presence of succinate plus rotenone, H_2O_2 produced by mitochondria from Wt mice was dramatically increased. Importantly, mitochondria from Tg(PRDX3) mice produced significantly reduced amount of H_2O_2 with these substrates relative to the amount of H_2O_2 produced from mitochondria from Wt mice, indicating that increased expression of Prdx3 decreases H_2O_2 production. To determine whether overexpression of Prdx3 affects mitochondria function, we also compared ATP production and membrane potential of mitochondria from Tg(PRDX3) mice and control Wt mice. As shown in Figure 2C and 2D, there were no significant differences in ATP production and membrane potential between mitochondria isolated from brain tissues of Tg(PRDX3) mice and Wt mice. Mitochondria isolated from skeletal muscle tissues of Tg(PRDX3) and Wt mice also show no difference in ATP production and membrane potential (data not shown).

Reduced cellular ROS and oxidative damage in Tg(PRDX3) mice

Mitochondria are the major source of cellular ROS. To test whether high levels of Prdx3 can reduce the ROS production, we compared levels of intracellular ROS in fibroblasts from Tg(PRDX3) mice and Wt mice using a DCF fluorescence spectrophotometer method described by Kashino et al (2003). As shown in Figure 3A, fibroblasts from Tg(PRDX3) mice had a significantly reduced level of DCF fluorescence compared to fibroblasts from Wt mice, indicating that overexpression of Prdx3 reduces levels of ROS in these cells.

To determine whether overexpression of Prdx3 can reduce levels of oxidative damage, we compared the basal level of total F_2-isoprostanes in liver from Tg(PRDX3) mice and Wt mice that were 3 to 4 months of age. As shown in Figure 3B, Tg(PRDX3) mice showed significantly lower levels of F_2-isoprostanes compared to Wt mice.

We further tested whether Tg(PRDX3) mice showed lower levels of oxidative damage in their mitochondria. 4-HNE adduct levels in mitochondrial proteins from Tg(PRDX3) mice and control Wt mice were measured and compared. As shown in Figure 3C, mitochondria isolated from Tg(PRDX3) mice showed a lower level of protein-bound 4-HNE than mitochondria isolated from control Wt mice.

Increased stress resistance of fibroblasts from Tg(PRDX3) mice

To determine whether the overexpression of Prdx3 affected cellular response to stress, we compared the sensitivities of fibroblasts from Tg(PRDX3) and Wt mice to several different agents that may cause cell death by elevated oxidative stress. Paraquat causes cell death by generation of intracellular superoxide (Bus et al., 1976; Cocheme and Murphy, 2008), while the toxicity of hydrogen peroxide is primarily ascribed to lipid peroxidation, lipid membrane perturbation, and its subsequent dissociation into hydroxyl and superoxide radicals (Halliwell and Gutteridge, 1989). The cytotoxicity of several metals, including cadmium, has been shown to be partly due to the generation of ROS (Stohs and Bagchi, 1995; Salmon

et al., 2005). The LD50 (lethal dose, 50%) value for each agents was determined as previously described by Salmon et al (2005). Compared to fibroblasts from Wt mice, fibroblasts from Tg(PRDX3) mice have greater resistance to paraquat (Figure 4A), hydrogen peroxide (Figure 4B) and cadmium (Figure 4C) as measured by the LD50 of cell lines isolated from 3–6 individual animals of each genotype. Thus, the overexpression of Prdx3 can increase cellular resistance to oxidative stress. Cells from Tg(PRDX3) mice were also resistant to tert-butyl hydrogen peroxide (t-BOOH) as measured by activation of caspase-3. As indicated in Figure 4D, treatment of t-BOOH resulted in an increase in level of activated caspase-3 in both Wt and Tg(PRDX3) cells. However, fibroblasts from Tg(PRDX3) mice showed reduced levels of activated caspase-3 compared to fibroblasts from Wt mice, indicating that oxidative stress-induced apoptosis was suppressed by overexpression of Prdx3.

Reduced plasma glucose and increased glucose clearance in Tg(PRDX3) mice

Tg(PRDX3) mice develop normally and there were no difference in bodyweight between Wt mice and Tg(PRDX3) mice up to 6 months of age (data not shown). Mitochondrial ROS are implicated to be important in the pathogenesis of diabetes (Houstis et al., 2006); to determine whether reduction in mitochondrial H_2O_2 affects glucose metabolism, we measured the basal and fasting blood glucose levels in Tg(PRDX3) and Wt mice. As shown in Figure 5A, Tg(PRDX3) mice had significantly reduced fasting glucose levels compared to Wt mice. We also compared insulin levels between Tg(PRDX3) and Wt mice. As shown in Figure 5B, there were no differences in serum insulin levels between Tg(PRDX3) and Wt mice, indicating that the reduced blood glucose in Tg(PRDX3) mice was not a result of elevated insulin level. Because glucose intolerance plays an important role in development of insulin resistance and diabetes, we also compared glucose tolerance between Tg(PRDX3) mice and Wt mice. As shown in Figure 5C, Tg(PRDX3) mice had significantly lower levels of blood glucose than Wt mice at all time points investigated after glucose administration, indicating that Tg(PRDX3) mice have increased glucose clearance.

Mitochondria ROS has been implicated as an important mediator of glucose intolerance and insulin resistance in diabetes (Houstis et al., 2006; Green et al., 2004). In mice, glucose metabolism can be impaired experimentally by feeding a diet high in dietary fat (Winzell and Ahren, 2004); so, to determine whether reduction in mitochondria H_2O_2 could lead to protection against hyperglycemia and glucose intolerance in Tg(PRDX3) mice, we fed Tg(PRDX3) mice and control Wt mice a high-fat diet (HFD) for 8 weeks. No differences in bodyweight and body fat content were observed between Tg(PRDX3) mice and Wt mice after HFD feeding (data not shown). At the end of the HFD feeding, we measured the basal and fasting blood glucose levels in Tg(PRDX3) and Wt mice. As shown in Figure 5D, HFD feeding increased blood glucose levels in Wt mice. Importantly, compared to HFD-fed Wt mice, HFD-fed Tg(PRDX3) mice had significantly reduced blood glucose levels both at fed and fasting conditions. As shown in Figure 5E, HFD-fed Tg(PRDX3) mice had reduced serum insulin levels at both fed and fasting conditions compared to HFD-fed Wt mice, indicating that the reduced glucose was not a result of elevated insulin level. We also compared glucose tolerance between HFD-fed Tg(PRDX3) mice and HFD-fed Wt mice (Figure 5F). HFD-feeding induced glucose intolerance in Wt mice; however, as with mice

fed a normal diet, we found that HFD-fed Tg(PRDX3) showed lower blood glucose levels relative to HFD-fed Wt mice at all time points measured following glucose administration. Thus, these results suggest that Tg(PRDX3) mice were protected from HFD-induced hyperglycemia and glucose intolerance.

Inhibition of GSK3 in Tg(PRDX3) mice

The PI3K/Akt signaling pathway is the classic signaling pathway mediating insulin-stimulated glucose usage and uptake. H_2O_2 is an important modulator of cell signaling and previous *in vitro* studies suggest that H_2O_2 may modulate the activation of this signaling pathway (Kwon et al., 2004). To address whether alteration of the PI3K/Akt signaling pathway played a role in mediating the improved glucose homeostasis phenotype in Tg(PRDX3) mice, we measured the levels of phosphorylated Akt in liver tissues of Tg(PRDX3) mice and Wt mice. As shown in Figure 6A and Figure 6B, Tg(PRDX3) mice had significantly increased levels of phosphorylated Akt compared to Wt mice.

GSK3 is a downstream target of Akt playing an important role in regulating glucose homeostasis (Lee and Kim, 2007). Phosphorylation of serine residues in GSK3 (ser-9 for GSK3β and ser-21 for GSK3α) by Akt inhibits GSK3 kinase activity, and inhibition of GSK3 has been shown to decrease blood glucose levels and to increase glucose clearance rates (Cline et al., 2002; Ring et al., 2003). To determine whether increased activation of Akt is correlated with inhibition of GSK3 in Tg(PRDX3) mice, we compared levels of phosphorylated GSK3β and levels of phosphorylated GSK3α in liver tissues from Tg(PRDX3) mice and Wt mice by Western blots. As shown in Figure 6C-6E, livers from Tg(PRDX3) mice had increased levels of phosphorylated GSK3β and GSK3α, suggesting that the activation of Akt resulted in inhibition of GSK3 in Tg(PRDX3) mice. After feeding a HFD diet, Tg(PRDX3) mice also showed increased phosphorylation of GSK3 that was correlated with activation of Akt (data not shown). Thus, the inhibition of GSK3 may play a role in mediating the improved glucose homeostasis phenotype in Tg(PRDX3) mice.

Discussion

Mitochondria are the major source of cellular ROS. During oxidative phosphorylation, electrons can escape from the mitochondrial electron transport complexes (ETC), especially from complexes I and III, and react with O_2 to form $O_2^{\bullet-}$ (Balaban et al., 2005). $O_2^{\bullet-}$ is subsequently converted to H_2O_2 by MnSOD and Cu/ZnSOD. It was estimated that up to 2% of the oxygen consumed by mitochondria is partially reduced to form $O_2^{\bullet-}$, which is subsequently converted to H_2O_2 (Chance et al., 1979), although more recent determinations have reduced this value to between 0.1% and 0.5% (Bayne et al., 2005). Unlike $O_2^{\bullet-}$, which can not cross the mitochondrial membranes because of its negative charge (Takahashi and Asada, 1983; Gus'kova et al., 1984), mitochondrial H_2O_2 readily diffuses through membranes, thereby producing bio-physiological effects both inside and outside of mitochondrion. Although H_2O_2 itself is only mildly reactive, H_2O_2 can react with transition metal such as Fe^{2+} through the Fenton reaction to generate hydroxyl radical ($OH^{\bullet-}$), which is highly reactive and can induce oxidative damage to DNA, protein and lipids. H_2O_2 also plays an important role in redox signaling through its ability to directly oxidize the redox-

active cysteinyl thiol in various target proteins (Stone and Yang, 2006). Recent data suggest that reduction in mitochondria H_2O_2 may be beneficial in retarding aging and diseases (Giorgio et al., 2007). For example, Schriner et al (2005) showed that transgenic mice overexpressing catalase in mitochondria had significant extension of lifespan, and Anderson et al (2008) showed that overexpression of catalase in mitochondria and overexpression of mitochondrial peroxidredoxin rescues frataxin deficiency in a *Drosophila* model of Friedreich's ataxia. However, the cellular and physiological roles of mitochondrial H_2O_2 were not fully explored in those studies. In addition, although overexpression of catalase in mitochondria by genetic engineering is effective in quenching H_2O_2, catalase is not a mitochondrial protein, thereby preventing it from being used as a cellular target for reducing mitochondrial H_2O_2. Prdx3 is a peroxiredoxin exclusively localized in mitochondria. In this report, we generated Tg(PRDX3) mice to determine whether mitochondrial H_2O_2 production can be quenched *in vivo* by overexpressing this native mitochondrial protein and to further understand the role of mitochondria H_2O_2 in aging and pathogenesis of diseases. Our results show that increased Prdx3 expression in Tg (PRDX3) mice leads to significantly reduced levels of H_2O_2 produced by mitochondria. Therefore, our results indicate that an increase in Prdx3 level is effective in reducing mitochondrial H_2O_2 *in vivo* and suggests that the Tg(PRDX3) mouse is a useful animal model in studying the cellular and physiological mechanisms of reduced mitochondrial H_2O_2 in aging and diseases.

Our data show that fibroblasts from Tg(PRDX3) mice have reduced cellular ROS and that tissues from Tg(PRDX3) mice have reduced levels of F_2-isoprostanes. Our results further show that mitochondria from Tg(PRDX3) have reduced 4-HNE protein adducts. Thus, our results indicate that overexpression of Prdx3 in mitochondria is effective in decreasing cellular ROS and oxidative damage. Our data also show that skin fibroblasts from Tg(PRDX3) mice have increased resistance to a variety of stressors. Previous results from immortal cell lines by other groups show that over-expression of Prdx3 leads to increased resistance to apoptosis and that knockdown of Prdx3 leads to increased sensitivity to apoptosis (Chang et al., 2004; Matsushima et al., 2006; Hattori et al., 2003). Thus, our results are consistent with these previous results, indicating that mitochondria H_2O_2 plays an important role in induction of apoptosis and that reduction in mitochondrial H_2O_2 by overexpression of Prdx3 is anti-apoptotic.

Metabolic changes that affect glucose homeostasis and insulin sensitivity are believed to be important in the development of diabetes and aging (Chang and Halter, 2003; Facchini et al., 2001; Barzilai et al., 1998). ROS has been implicated to play a role in regulating glucose metabolism and insulin sensitivity (Houstis et al., 2006); however, whether reduction in mitochondrial H_2O_2 can directly lead to change in glucose metabolism is unclear. Our results show that Tg(PRDX3) mice had reduced fasting glucose levels and increased glucose clearance. Therefore, overexpression of Prdx3 improves glucose metabolism in Tg(PRDX3) mice. Because the direct result of Prdx3 overexpression is reduced mitochondrial H_2O_2 production, our data suggest that reducing mitochondrial H_2O_2 can lead to change in glucose homeostasis. Mitochondria ROS is believed to be important in pathogenesis of diabetes (Nishikawa and Araki, 2007), and reduction in mitochondria ROS is proposed to be a therapeutic strategy in diabetes (Houstis et al., 2006; Green et al., 2004). In this study, we

show that Tg(PRDX3) mice are protected against glucose metabolism impairment induced by high-fat diet feeding. Interestingly, a previous study showed that transgenic mice overexpressing Gpx1 develop hyperglycemia and obesity (McClung et al., 2004). Although a small portion of Gpx1 is present in mitochondria, the majority of Gpx1 is located in cytosol (Panfili et al., 1991; Esworthy et al., 1997; Ho et al., 1997). Therefore, the different phenotypes observed between the Gpx1 transgenic mice and Tg(PRDX3) mice may arise from differences in subcellular locations of Gpx1 and Prdx3. Our results from Tg(PRDX3) mice suggest that decreasing H_2O_2 in mitochondria may be a therapeutic/preventive strategy in diabetes. Glucose intolerance is associated with aging (DeFronzo, 1981), and calorie restriction, a manipulation that retards aging, improves glucose tolerance (Weiss and Holloszy, 2007). Reduction of mitochondria H_2O_2 through transgenic overexpression of mitochondrially-targeted catalase has also been shown to retard aging (Schriner et al., 2005), Thus, it seems that mitochondrial H_2O_2 is important for both the regulation of aging and age-related diseases and it will therefore be important to determine whether Tg(PRDX3) mice are long-lived.

We also investigated the potential mechanisms by which reduced mitochondrial H_2O_2 may leads to improved glucose homeostasis. The phosphatidyinositol 3 kinase (PI3K)/Akt pathway is responsible for insulin-stimulated glucose storage and uptake. Although there was no difference in insulin levels between Tg(PRDX3) mice and control Wt mice, Tg(PRDX3) mice showed increased level of phosphorylated Akt, indicating that Akt is activated in Tg(PRDX3) mice. GSK3 is a downstream target of PI3K/Akt signaling pathway that plays a very important role in regulating glucose homeostasis. Our result showed that Tg(PRDX3) mice have increased phosphorylation of GSK3β and GSK3α. Thus, activation of Akt appears to lead to increased phosphorylation of GSK3, thereby inhibition of GSK3 activity in Tg(PRDX3) mice. Previous studies show that inhibition of GSK3 pharmacologically with GSK3 inhibitors reduces blood glucose level and increases glucose disposal in diabetes-prone Zucker diabetic fatty rats and *db/db* mice (Cline et al., 2002; Ring et al., 2003; Kaidanovich-Beilin and Eldar-Finkelman, 2006). Thus, our results suggest that improved glucose homeostasis phenotype in Tg(PRDX3) mice may be partially mediated by activation of Akt and the resultant inhibition of GSK3 activity. The mechanism by which reduced mitochondria H_2O_2 may lead to activation of Akt is unclear at present. Interestingly, previous studies show that increased H_2O_2 level activate the PI3K/Akt signaling pathway and that the mechanism of H_2O_2- induced activation of PI3K/Akt involves inhibiting the activity of protein-tyrosine phosphatases (PTPs) conferred by oxidation of cysteine residues of PTPs by H_2O_2 (Salmeen et al., 2003; van Montfort et al., 2003). Our observation that reduction of H_2O_2 leads to activation of Akt in Tg(PRDX3) mice appears to go against this model of cell signaling induced by H_2O_2. However, the signaling in Tg(PRDX3) mice was initiated from reduced level of endogenous H_2O_2, which is lower than the concentrations of H_2O_2 used in many of the *in vitro* studies (Salmeen et al., 2003). It is known that there are many PTPs (Alonso et al., 2004; Andersen, 2004) and each PTP appears to have different susceptibility to oxidation (Groen et al., 2005). Under the reduced level of H_2O_2 in Tg(PRDX3) mice, activation of Akt could result from activation or deactivation of a different set of PTPs. Thus, our observation that reduced H_2O_2 activates Akt may not be irreconcilable with the classic model. Alternatively, reduction in H_2O_2 could

lead to activation of Akt through mechanisms other than deactivation of PTPs, such as redox regulation of transcription factors (Veal et al., 2007). Tg(PRDX3) mice may allow us to investigate the signaling pathways modulated by H_2O_2 *in vivo* and to understand consequences of H_2O_2 action under physiological conditions.

In summary, we generated a novel transgenic mice model overexpressing Prdx3 in mitochondria. We showed that overexpression of PRDX3 resulted in significant reduction of H_2O_2 produced by mitochondria and as a result of reduced H_2O_2 production by mitochondria, Tg(PRDX3) mice show low level of oxidative damage and cells from Tg(PRDX3) mice exhibit increased resistance to stress. More importantly, Tg(PRDX3) mice show improved glucose homeostasis and are protected against hyperglycemia and glucose intolerance induced by HFD feeding. Therefore, our results indicate that reduction in mitochondrial H_2O_2 could be beneficial for therapy and prevention of diseases such as diabetes.

Experimental Procedures

Animals

The BAC clone CTD-2537P4 containing the entire human PRDX3 gene was obtained from Invitrogen Co. (Carlsbad, CA). The presence of PRDX3 gene and 5′ and 3′ flanking sequences was confirmed by restriction digestion, Southern blot and PCR analysis. The *SbfI* fragment (34.4 kb) of this BAC clone contains the intact human PRDX3 gene (approximately 11 kb) plus approximately 16.5 kb and 6.7 kb of 5′- and 3′-flanking sequences, respectively. This fragment was isolated and used to generate transgenic mice. The transgenic mice were generated in B6SJL F1 background at the Transgenic Core of the University of Michigan. A PCR based genotyping protocol was used to genotype the mice with the human PRDX3 gene using forward primer (AGC TTC TGA TCA ACG GTC CT) and reverse primer (ATT TCA GGG ATG AGG GAT CA). The Tg(PRDX3) mice were subsequently backcrossed two generations to C57/B6J mice. The Tg(PRDX3) mice used in this study were in a mixed background of B6 and SJL. The control wildtype were littermates of Tg(PRDX3) mice. Male and female mice that were 2 to 3 months of age were used for measuring expression, mitochondrial H_2O_2 and oxidative damage. Female mice that were 2 to 4 months of age were used for glucose metabolism study and high-fat diet feeding study. The group sizes for each study were indicated in the results.

All procedures for handling the mice in this study were reviewed and approved by the IACUC (Institutional Animal Care and Use Committee) of University of Texas Health Science Center at San Antonio (UTHSCSA) and the IACUC of South Texas Veterans Health Care System, Audie Murphy VA Hospital.

RNA isolation and RT-PCR

Total RNA was isolated from tissues using Tri Reagent (Molecular Research Center, Cincinnati, OH) according to the manufacturer's instructions. Total RNA (1 μg) from Tg(PRDX3) mice and Wt mice was reverse-transcribed using random hexamers and Multi-Scribe Reverse Transcriptase (Applied Biosystems, Foster City, CA). Quantitative real-time

PCR was performed to determine total Prdx3 mRNA levels using the following PCR primers: Prdx3-1f (GTG TGT CCT ACA GAA ATT GTT) and Prdx3-1r (AAC CAC CAT TCT TCC TTG GTG). Quantitative real-time PCR was performed with the SYBR Green detection system (Applied Biosystems) using an ABI Prism 7500 sequence detector and under thermal cycling conditions of preincubation (50°C, 2 min); DNA polymerase activation (95°C, 10 min); and 40 PCR cycles for 15 s at 95°C, and 1 min at 60°C. The mRNA levels were normalized to beta-actin to control for input RNA. The mean levels of Prdx3 mRNA in Wt mice were assigned as 1 arbitrarily, and relative levels of Prdx3 mRNA were presented as means ± SEM.

Subcellular fractionation

Liver tissues were homogenized in buffer 1 (250 mM Mannitol, 75 mM Sucrose, 500 μM EGTA, 100 μM EDTA, and 10 mM Hepes, pH 7.4) supplemented with protease inhibitor cocktail. The homogenates were centrifuged at 600g for 10 min at 4°C to pellet nuclei and unbroken cells. The resultant supernatant was then centrifuged at 10,000g for 10 min at 4°C to obtain the mitochondria pellet. The supernatant was further centrifuged at 100, 000g for 60 min at 4°C to yield the cytosol. Prdx3 protein levels in each fraction were determined by Western blots. ATPase was used as a mitochondria marker, whereas β-tublin was used as a cytosol marker.

Immunostaining and confocal-microscopy

Skin fibroblasts from Tg(PRDX3) mice and Wt mice were isolated and cultured using methods similar to those described by Salmon et al (2005). Briefly, tail skin biopsies were obtained from the latter half of the intact tail of isoflurane-anesthetized mice after skin sterilization with 70% ethanol. Biopsies were then diced and digested overnight with collagenase type II (400 U/ml, 1,000 U total per tail, GIBCO-Invitrogen) dissolved in DMEM supplemented with 10% heat-inactivated fetal bovine serum, antibiotics (100 U/ml penicillin and 100 μg/ml streptomycin; Sigma, St. Louis, MO), and 0.25 μg/ml fungizone (Biowhittaker-Cambrex Life Sciences, Walkersville, MD). After collagenase treatment, cells were resuspended in DMEM with 20% heat inactivated fetal bovine serum, antibiotics, and fungizone and seeded into tissue culture flasks of 25 cm^2 surface area. All subsequent cell subcultures were grown in this media and all cultures were grown at 37° C in a humidified incubator with 5% CO2 in air.

For co-localization study, fibroblasts were firstly loaded with MitoTracker red to label mitochondria. After fixation, the cells were sequentially stained with anti-Prdx3 antibody and with an Alexa488-labeled secondary antibody. The confocal microscopy images of Prdx3 staining (green) and mitochondria (red) were taken using a Zeiss confocal LSM 510 microscope.

Assays for mitochondria H_2O_2, ATP production and membrane potential

Mitochondria were isolated from whole hindlimb skeletal muscle and brain, as described previously (Muller et al., 2007). Briefly, hindlimb skeletal muscle was excised, weighed, bathed in 150 mM KCl, and placed in Chappell-Perry buffer with the protease nagarse. The minced skeletal muscle was homogenized, and the homogenate was centrifuged for 10 min

at 600 *g*, with the supernatant then being passed through cheesecloth and centrifuged at 14,000 *g* for 10 min. The resultant pellet was washed once in modified Chappell-Perry buffer with 0.1% fatty acid free BSA and twice in modified Chappell-Perry buffer without bovine serum albumin. Mitochondria from whole brain were isolated by homogenization followed by two-step centrifugation: 10 min at 1000 *g* to remove unbroken cells/tissue and at 10,000 *g* for 10 min to pellet the mitochondria. Protein concentration was measured with the Bradford method.

Freshly isolated mitochondria were used for H_2O_2 release assay with the amplex red-horseradish peroxidase (HRP) method (Zhou et al., 1997; Muller et al., 2007). HRP (1 U/ml) catalyzes the H_2O_2-dependent oxidation of nonfluorescent Amplex red (80 μM) (Molecular Probes, Eugene, OR) to fluorescent resorufin red. Fluorescence was followed at an excitation wavelength of 544 nm and emission wavelength of 590 nm using a Fluoroskan Ascent type 374 multiwell plate reader (Labsystems, Helsinki, Finland). The slope of the increase in fluorescence is converted to the rate of H_2O_2 production with a standard curve. All assays were performed at 37°C in 96-well plates. Substrates used were 10 mM succinate plus rotenone and 5 mM glutamate plus malate. For each assay, one reaction well contained buffer only, and another contained buffer with mitochondria, to estimate the background oxidation rates of Amplex red and to estimate the rate of H_2O_2 release in mitochondria without substrate (state 1). The reaction buffer consisted of 125 mM KCl, 10 mM HEPES, 5 mM $MgCl_2$, 2 mM K_2HPO4, pH 7.44 and 37.5 U/ml of Sod.

ATP production was measured using a luciferase/luciferin based system as described Drew and Leeuwenburgh (Drew and Leeuwenburgh, 2003). Mitochondria in reaction buffer were incubated with either 5 mM malate plus pyruvate or 10 mM succinate plus 1 μM rotenone and a buffer containing 0.8 mM luciferin/20 mg/ml luciferase and 0.3 mM ADP. The rate of mitochondrial ATP synthesis is expressed as nmol ATP per minute per mg mitochondrial protein.

The mitochondrial membrane potential was measured by safranin O uptake into the mitochondria as previously described (Feldkamp et al., 2005; Vercesi et al., 1991) with the following modifications: 5 μg of mitochondria protein was added into 100 ul reaction buffer containing 5 μM safranin O. After 5 minutes of incubation with substrates as above described, the fluorescence was followed at 485-nm excitation, 590-nm emission using a Fluoroskan Ascent (Labsystems, Finland). The safranin O uptake was calculated as the change in fluorescence between the reaction buffer without and with mitochondria.

Measurement of F_2-isoprostanes

Levels of F_2-isoprostanes in liver were determined as described by Morrow and Roberts (Morrow and Roberts, 1999). Briefly, F_2-isoprostanes were extracted and quantified by GC/MS using the internal standard, [$^2H_4$] 8-Iso-$PGF_{2\alpha}$, which was added to the samples at the beginning of extraction to correct yield of the extraction process. The amount of F_2-isoprostanes in liver was expressed as pg of 8-Iso-$PGF_{2\alpha}$ per mg of total liver protein.

Cellular stress resistance assay

The cytotoxicity assay was conducted as described by Salmon et al (2005). Briefly, cells were exposed to a range of doses of one of the cytotoxic stressors. Cells were then incubated in DMEM supplemented with 2% BSA, antibiotics, and fungizone, and their survival was measured 18 h later by a test based on oxidative cleavage of the tetrazolium dye WST-1 (Roche Applied Science, Indianapolis, IN) to a formazan product, using the protocol suggested by the manufacturer. At each dose of chemical stressor, mean survival was calculated for triplicate wells for each cell line. The LD50, i.e., dose of stress agent that led to survival of 50% of the cells, was then calculated using probit analysis as implemented in NCSS software (NCSS, Kaysville, UT).

Caspase-3 protein levels in fibroblasts were determined by Western blot using an anti-caspase-3 antibody (sc-7148, Santa Cruz Biotechnology, Inc., CA). The intensities of bands corresponding to p20 of caspase-3 (the subunit of activated caspase-3) were used as indicators of caspase-3 activation.

Blood glucose and insulin measurement and glucose tolerance test

Blood was collected from the tail vein of fed mice (basal) and fasting mice (for 18 hrs) and glucose level was measured using as One-touch hand-held glucometer. The plasma insulin level was measured using the Insulin (Mouse EIA) kit from ALPCO Diagnostics (Salem, NH). For glucose tolerance test, mice were deprived of food overnight (18 hrs), after which an intraperitoneal injection of dextrose (1mg/g) was administrated to mice at time zero. Tail vein blood samples were collected for glucose analysis at the indicated time points, and glucose level was measured as above descibed.

High-fat diet feeding

Female mice that were 8–9 weeks of age were fed a high-fat diet (Research Diets, New Brunswick, NJ) for 8 weeks. On caloric basis, the high-fat diet consisted of 58% fat from lard, 25.6% carbohydrate, and 16.4% protein (total 23.4 kJ/g).

Western blots

4-HNE measurement: Levels of 4-HNE protein adducts in isolated mitochondria were measured by Western blots. Briefly, mitochondria from liver tissues were homogenized in a RIPA buffer (20 mM Tris, pH7.4, 0.25 M NaCl, 1 mM EDTA, 0.5% NP-40, 50 mM sodium fluoride) supplemented with protease inhibitors. Equal amounts of total proteins (20 μg) were separated by 4–20% SDS-PAGE and transferred to nitrocellulose membranes. The membranes were blocked for 1 hour in 5% nonfat dry milk and were incubated for 2 hours at room temperature with an anti-4-HNE monoclonal antibody (MAB3249, R&D Systems, Inc., Minneapolis, MN). 4-HNE adducts bands were scanned and quantified using ImageQuant software (Molecular Dynamics, Sunnyvale, CA).

Prdx3 protein: Prdx3 protein levels in tissues from Tg(PRDX3) and Wt mice were determined by Western blots using an anti-Prdx3 antibody that recognizes both mouse and human Prdx3 protein (Ab16751 from Abcam, Inc., Cambridge, MA).

Akt and GSK3: Liver tissues were homogenized in a RIPA buffer with protease inhibitors and phosphotases inhibitors. The levels of phosphorylated Akt and GSK3α and GSK3β proteins were determined using antibodies specific to phosphorylated proteins and total proteins obtained from Cell Signaling Technology, Inc. (Danvers, MA). The following antibodies were used: anti-phospho-Akt (ser473) (Cat#4058); anti-Akt (Cat# 9272); anti-phospho-GSK3α (Ser21) (Cat#9316); anti-GSK3α (Cat# 9338); anti-phospho-GSK3β (Ser9) (Cat#9336); anti-GSK3β(Cat# 9315);

Statistical Analysis

Data are expressed as mean ± SEM as indicated in the figures. Results were statistically analyzed using two-way ANOVA or Student's *t* test when appropriate. Statistical significance is set to a minimum of $p<0.05$.

Acknowledgments

The study was supported by a Merit Award (Q.R.) from the Department of Veteran Affairs and a Nathan Shock Center award (A.R.) from NIA/NIH.

References

Alonso A, Sasin J, Bottini N, Friedberg I, Friedberg I, Osterman A, Godzik A, Hunter T, Dixon J, Mustelin T. Protein tyrosine phosphatases in the human genome. Cell. 2004; 117:699–711. [PubMed: 15186772]

Ames BN, Shigenaga MK, Hagen TM. Mitochondrial decay in aging. Biochim Biophys Acta Mol Basis Dis. 1995; 1271:165–170.

Andersen JK. Oxidative stress in neurodegeneration: cause or consequence? Nat Med. 2004; 10(Suppl):S18–S25. [PubMed: 15298006]

Anderson PR, Kirby K, Orr WC, Hilliker AJ, Phillips JP. Hydrogen peroxide scavenging rescues frataxin deficiency in a Drosophila model of Friedreich's ataxia. Proc Natl Acad Sci U S A. 2008; 105:611–616. [PubMed: 18184803]

Balaban RS, Nemoto S, Finkel T. Mitochondria, oxidants, and aging. Cell. 2005; 120:483–495. [PubMed: 15734681]

Barzilai N, Banerjee S, Hawkins M, Chen W, Rossetti L. Caloric restriction reverses hepatic insulin resistance in aging rats by decreasing visceral fat. J Clin Invest. 1998; 101:1353–1361. [PubMed: 9525977]

Bayne AC, Mockett RJ, Orr WC, Sohal RS. Enhanced catabolism of mitochondrial superoxide/hydrogen peroxide and aging in transgenic Drosophila. Biochem J. 2005; 391:277–284. [PubMed: 15954861]

Brigelius-Flohe R. Tissue-specific functions of individual glutathione peroxidases. Free Radic Biol Med. 1999; 27:951–965. [PubMed: 10569628]

Bus JS, Cagen SZ, Olgaard M, Gibson JE. A mechanism of paraquat toxicity in mice and rats. Toxicol Appl Pharmacol. 1976; 35:501–513. [PubMed: 1265764]

Cao Z, Bhella D, Lindsay JG. Reconstitution of the mitochondrial PrxIII antioxidant defence pathway: general properties and factors affecting PrxIII activity and oligomeric state. J Mol Biol. 2007; 372:1022–1033. [PubMed: 17707404]

Chae HZ, Kim HJ, Kang SW, Rhee SG. Characterization of three isoforms of mammalian peroxiredoxin that reduce peroxides in the presence of thioredoxin. Diabetes Res Clin Pract. 1999; 45:101–112. [PubMed: 10588361]

Chance B, Sies H, Boveris A. Hydroperoxide metabolism in mammalian organs. Physiol Rev. 1979; 59:527–605. [PubMed: 37532]

Chang AM, Halter JB. Aging and insulin secretion. Am J Physiol Endocrinol Metab. 2003; 284:E7–12. [PubMed: 12485807]

Chang TS, Cho CS, Park S, Yu S, Kang SW, Rhee SG. Peroxiredoxin III, a mitochondrion-specific peroxidase, regulates apoptotic signaling by mitochondria. J Biol Chem. 2004; 279:41975–41984. [PubMed: 15280382]

Cline GW, Johnson K, Regittnig W, Perret P, Tozzo E, Xiao L, Damico C, Shulman GI. Effects of a novel glycogen synthase kinase-3 inhibitor on insulin-stimulated glucose metabolism in Zucker diabetic fatty (fa/fa) rats. Diab. 2002; 51:2903–2910.

Cocheme HM, Murphy MP. Complex I is the major site of mitochondrial superoxide production by paraquat. J Biol Chem. 2008; 283:1786–1798. [PubMed: 18039652]

DeFronzo RA. Glucose intolerance and aging. Diabetes Care. 1981; 4:493–501. [PubMed: 7049632]

Drew B, Leeuwenburgh C. Method for measuring ATP production in isolated mitochondria: ATP production in brain and liver mitochondria of Fischer-344 rats with age and caloric restriction. Am J Physiol Regul Integr Comp Physiol. 2003; 285:R1259–R1267. [PubMed: 12855419]

Esworthy RS, Ho YS, Chu FF. The Gpx1 gene encodes mitochondrial glutathione peroxidase in the mouse liver. Arch Biochem Biophys. 1997; 340:59–63. [PubMed: 9126277]

Facchini FS, Hua N, Abbasi F, Reaven GM. Insulin resistance as a predictor of age-related diseases. J Clin Endocrinol Metab. 2001; 86:3574–3578. [PubMed: 11502781]

Feldkamp T, Kribben A, Weinberg JM. Assessment of mitochondrial membrane potential in proximal tubules after hypoxia-reoxygenation. Am J Physiol Renal Physiol. 2005; 288:F1092–F1102. [PubMed: 15625081]

Giorgio M, Trinei M, Migliaccio E, Pelicci PG. Hydrogen peroxide: a metabolic by-product or a common mediator of ageing signals? Nat Rev Mol Cell Biol. 2007; 8:722–728. [PubMed: 17700625]

Green K, Brand MD, Murphy MP. Prevention of mitochondrial oxidative damage as a therapeutic strategy in diabetes. Diab. 2004; 53(Suppl 1):S110–S118.

Groen A, Lemeer S, van der WT, Overvoorde J, Heck AJ, Ostman A, Barford D, Slijper M, Den Hertog J. Differential oxidation of protein-tyrosine phosphatases. J Biol Chem. 2005; 280:10298–10304. [PubMed: 15623519]

Gus'kova RA, Ivanov II, Kol'tover VK, Akhobadze VV, Rubin AB. Permeability of bilayer lipid membranes for superoxide (O2-) radicals Biochim Biophys Acta. 1984; 778:579–585.

Halliwell, B.; Gutteridge, JMC. Free radicals in biology and medicine. Oxford: Oxford University Press; 1989.

Harman, D. The free-radical theory of aging. In: Warner, RN.; Butler, RL.; Sprott, RL.; Schneider, EL., editors. Modern Biological Theories of Aging. New York: Raven Press; 1987. p. 81-87.

Hattori F, Murayama N, Noshita T, Oikawa S. Mitochondrial peroxiredoxin-3 protects hippocampal neurons from excitotoxic injury in vivo. J Neurochem. 2003; 86:860–868. [PubMed: 12887684]

Ho YS, Magnenat JL, Bronson RT, Cao J, Gargano M, Sugawara M, Funk CD. Mice deficient in cellular glutathione peroxidase develop normally and show no increased sensitivity to hyperoxia. J Biol Chem. 1997; 272:16644–16651. [PubMed: 9195979]

Houstis N, Rosen ED, Lander ES. Reactive oxygen species have a causal role in multiple forms of insulin resistance. Nature. 2006; 440:944–948. [PubMed: 16612386]

Kaidanovich-Beilin O, Eldar-Finkelman H. Long-term treatment with novel glycogen synthase kinase-3 inhibitor improves glucose homeostasis in ob/ob mice: molecular characterization in liver and muscle. J Pharmacol Exp Ther. 2006; 316:17–24. [PubMed: 16169938]

Kashino G, Kodama S, Nakayama Y, Suzuki K, Fukase K, Goto M, Watanabe M. Relief of oxidative stress by ascorbic acid delays cellular senescence of normal human and Werner syndrome fibroblast cells. Free Radic Biol Med. 2003; 35:438–443. [PubMed: 12899945]

Krapfenbauer K, Engidawork E, Cairns N, Fountoulakis M, Lubec G. Aberrant expression of peroxiredoxin subtypes in neurodegenerative disorders. Brain Res. 2003; 967:152–160. [PubMed: 12650976]

Kwon J, Lee SR, Yang KS, Ahn Y, Kim YJ, Stadtman ER, Rhee SG. Reversible oxidation and inactivation of the tumor suppressor PTEN in cells stimulated with peptide growth factors. Proc Natl Acad Sci U S A. 2004; 101:16419–16424. [PubMed: 15534200]

Lee J, Kim MS. The role of GSK3 in glucose homeostasis and the development of insulin resistance. Diabetes Res Clin Pract. 2007; 77(Suppl 1):S49–S57. [PubMed: 17478001]

Lowell BB, Shulman GI. Mitochondrial dysfunction and type 2 diabetes. Science. 2005; 307:384–387. [PubMed: 15662004]

Matsushima S, Ide T, Yamato M, Matsusaka H, Hattori F, Ikeuchi M, Kubota T, Sunagawa K, Hasegawa Y, Kurihara T, Oikawa S, Kinugawa S, Tsutsui H. Overexpression of mitochondrial peroxiredoxin-3 prevents left ventricular remodeling and failure after myocardial infarction in mice. Circulation. 2006; 113:1779–1786. [PubMed: 16585391]

McClung JP, Roneker CA, Mu W, Lisk DJ, Langlais P, Liu F, Lei XG. Development of insulin resistance and obesity in mice overexpressing cellular glutathione peroxidase. Proc Natl Acad Sci U S A. 2004; 101:8852–8857. [PubMed: 15184668]

Morrow JD, Roberts LJ. Mass spectrometric quantification of F2-isoprostanes in biological fluids and tissues as measure of oxidant stress. Methods Enzymol. 1999; 300:3–12. [PubMed: 9919502]

Mukhopadhyay SS, Leung KS, Hicks MJ, Hastings PJ, Youssoufian H, Plon SE. Defective mitochondrial peroxiredoxin-3 results in sensitivity to oxidative stress in Fanconi anemia. J Cell Biol. 2006; 175:225–235. [PubMed: 17060495]

Muller FL, Song W, Jang YC, Liu Y, Sabia M, Richardson A, Van Remmen H. Denervation-induced skeletal muscle atrophy is associated with increased mitochondrial ROS production. Am J Physiol Regul Integr Comp Physiol. 2007; 293:R1159–R1168. [PubMed: 17584954]

Nishikawa T, Araki E. Impact of mitochondrial ROS production in the pathogenesis of diabetes mellitus and its complications. Antioxid Redox Signal. 2007; 9:343–353. [PubMed: 17184177]

Panfili E, Sandri G, Ernster L. Distribution of glutathione peroxidases and glutathione reductase in rat brain mitochondria. FEBS Lett. 1991; 290:35–37. [PubMed: 1915888]

Ran Q, Liang H, Gu M, Qi W, Walter CA, Roberts LJ, Herman B, Richardson A, Van Remmen H. Transgenic mice overexpressing glutathione peroxidase 4 are protected against oxidative stress-induced apoptosis. J Biol Chem. 2004; 279:55137–55146. [PubMed: 15496407]

Rhee SG. Cell signaling. H2O2, a necessary evil for cell signaling. Science. 2006; 312:1882–1883. [PubMed: 16809515]

Rhee SG, Chae HZ, Kim K. Peroxiredoxins: a historical overview and speculative preview of novel mechanisms and emerging concepts in cell signaling. Free Radic Biol Med. 2005; 38:1543–1552. [PubMed: 15917183]

Ring DB, Johnson KW, Henriksen EJ, Nuss JM, Goff D, Kinnick TR, Ma ST, Reeder JW, Samuels I, Slabiak T, Wagman AS, Hammond ME, Harrison SD. Selective glycogen synthase kinase 3 inhibitors potentiate insulin activation of glucose transport and utilization in vitro and in vivo. Diab. 2003; 52:588–595.

Salmeen A, Andersen JN, Myers MP, Meng TC, Hinks JA, Tonks NK, Barford D. Redox regulation of protein tyrosine phosphatase 1B involves a sulphenyl-amide intermediate. Nature. 2003; 423:769–773. [PubMed: 12802338]

Salmon AB, Murakami S, Bartke A, Kopchick J, Yasumura K, Miller RA. Fibroblast cell lines from young adult mice of long-lived mutant strains are resistant to multiple forms of stress. Am J Physiol Endocrinol Metab. 2005; 289:E23–E29. [PubMed: 15701676]

Schriner SE, Linford NJ, Martin GM, Treuting P, Ogburn CE, Emond M, Coskun PE, Ladiges W, Wolf N, Van Remmen H, Wallace DC, Rabinovitch PS. Extension of murine life span by overexpression of catalase targeted to mitochondria. Science. 2005; 308:1909–1911. [PubMed: 15879174]

Stohs SJ, Bagchi D. Oxidative mechanisms in the toxicity of metal ions. Free Radic Biol Med. 1995; 18:321–336. [PubMed: 7744317]

Stone JR, Yang S. Hydrogen peroxide: a signaling messenger. Antioxid Redox Signal. 2006; 8:243–270. [PubMed: 16677071]

Takahashi MA, Asada K. Superoxide anion permeability of phospholipid membranes and chloroplast thylakoids. Arch Biochem Biophys. 1983; 226:558–566. [PubMed: 6314906]

van Montfort RL, Congreve M, Tisi D, Carr R, Jhoti H. Oxidation state of the active-site cysteine in protein tyrosine phosphatase 1B. Nature. 2003; 423:773–777. [PubMed: 12802339]

Veal EA, Day AM, Morgan BA. Hydrogen peroxide sensing and signaling. Mol Cell. 2007; 26:1–14. [PubMed: 17434122]

Vercesi AE, Bernardes CF, Hoffmann ME, Gadelha FR, Docampo R. Digitonin permeabilization does not affect mitochondrial function and allows the determination of the mitochondrial membrane potential of Trypanosoma cruzi in situ. J Biol Chem. 1991; 266:14431–14434. [PubMed: 1860850]

Weiss EP, Holloszy JO. Improvements in body composition, glucose tolerance, and insulin action induced by increasing energy expenditure or decreasing energy intake. J Nutr. 2007; 137:1087–1090. [PubMed: 17374683]

Winzell MS, Ahren B. The high-fat diet-fed mouse: a model for studying mechanisms and treatment of impaired glucose tolerance and type 2 diabetes. Diab. 2004; 53(Suppl 3):S215–S219.

Wood-Allum CA, Barber SC, Kirby J, Heath P, Holden H, Mead R, Higginbottom A, Allen S, Beaujeux T, Alexson SE, Ince PG, Shaw PJ. Impairment of mitochondrial anti-oxidant defence in SOD1-related motor neuron injury and amelioration by ebselen. Brain. 2006; 129:1693–1709. [PubMed: 16702190]

Zhang H, Go YM, Jones DP. Mitochondrial thioredoxin-2/peroxiredoxin-3 system functions in parallel with mitochondrial GSH system in protection against oxidative stress. Arch Biochem Biophys. 2007; 465:119–126. [PubMed: 17548047]

Zhou M, Diwu Z, Panchuk-Voloshina N, Haugland RP. A stable nonfluorescent derivative of resorufin for the fluorometric determination of trace hydrogen peroxide: applications in detecting the activity of phagocyte NADPH oxidase and other oxidases. Anal Biochem. 1997; 253:162–168. [PubMed: 9367498]

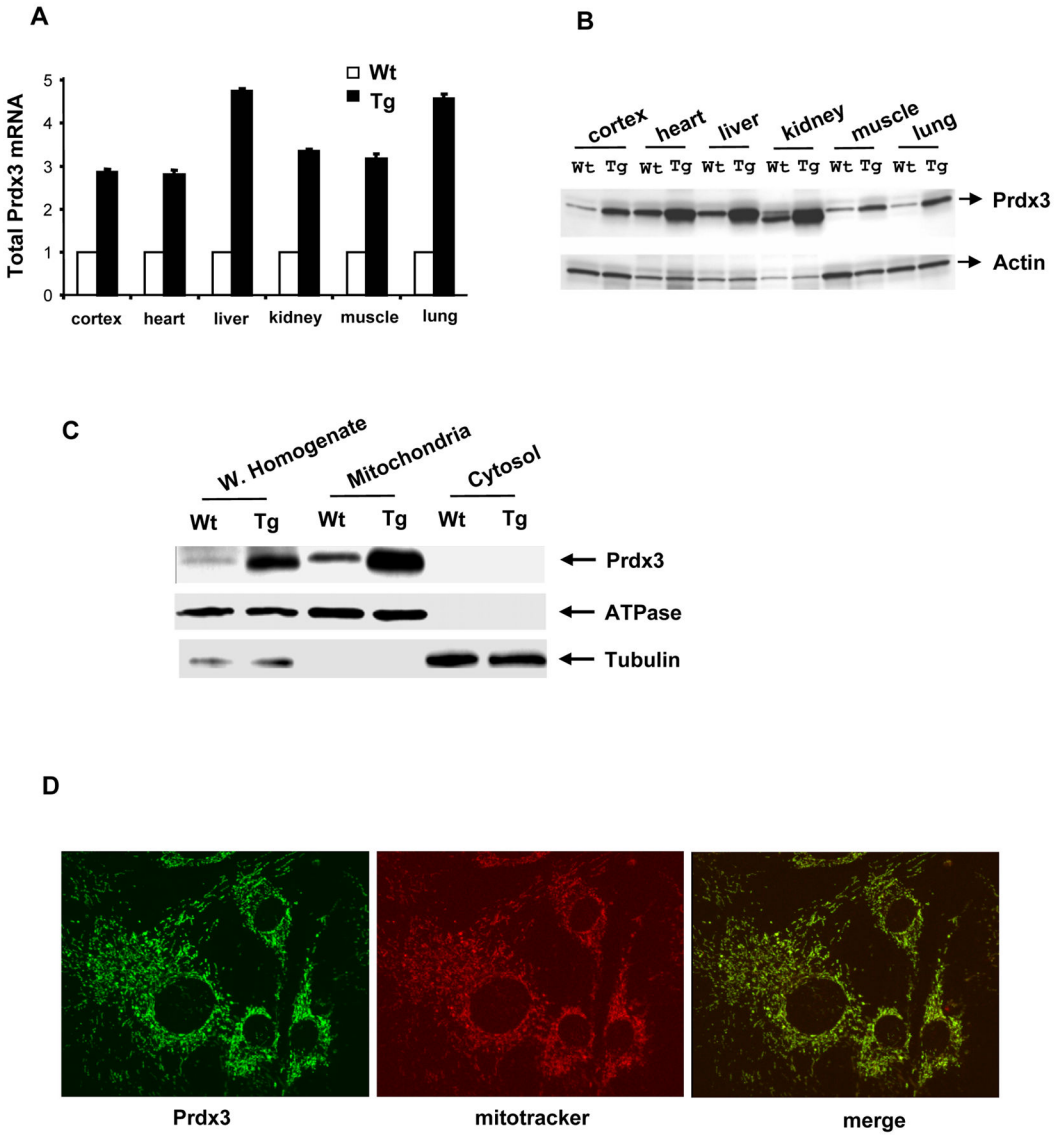

Figure 1. Increased level of Prdx3 in Tg(PRDX3) mice

A. Total Prdx3 mRNA levels in tissues from Tg(PRDX3) mice (Tg) and wildtype mice (Wt) were determined by quantitative Real-time PCR. The mean values obtained from Wt mice were artificially assigned as 1, and the relative values obtained from Tg mice are presented as mean ± SEM. n=3.

B. A graph of Western blot showing total Prdx3 protein levels in tissues from Tg(PRDX3) mice and Wt mice. The levels of beta-actin were used as loading controls.

C. Prdx3 protein levels in whole tissue homogenate, mitochondrial fraction and cytosolic fraction from livers of Tg(PRDX3) and Wt mice were measured by Western blot. Level of ATPase was used as a mitochondria marker, whereas β-tubulin was used as a cytosolic marker.

D. Localization of PRDX3 protein in mitochondria. Skin fibroblasts from Tg(PRDX3) mice were firstly loaded with MitoTracker red to label mitochondria and subsequently stained for Prdx3 protein. The imaging of Prdx3 staining (green), mitochondria (red) and co-

localization of Prdx3 and mitochondria (merge) were performed by confocal laser scanning microscopy.

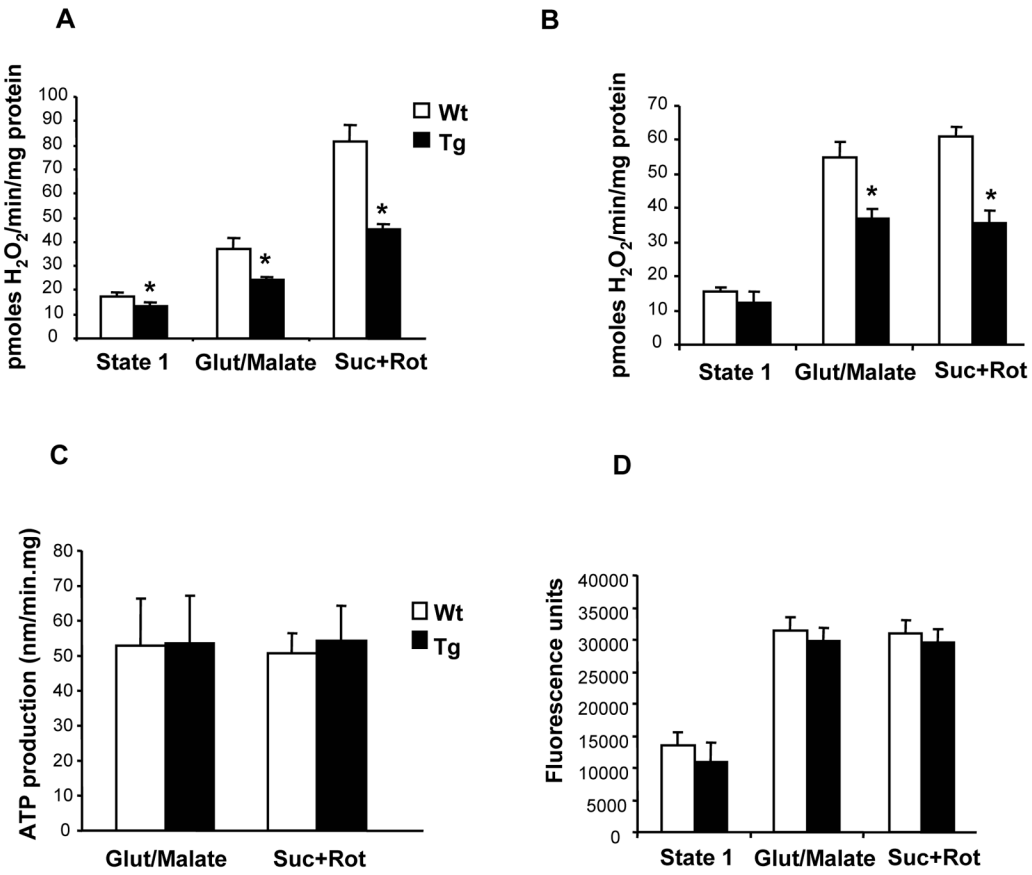

Figure 2. Reduced H_2O_2 production by mitochondria from Tg(PRDX3) mice

A. Levels of H_2O_2 produced by mitochondria isolated from brain were measured as described by Muller et al (2007b).

B. Levels of H_2O_2 produced by mitochondria isolated from skeletal muscle were measured as described by Muller et al (2007b).

C. Levels of ATP production by mitochondria isolated from brain were measured as described in Methods.

D. Mitochondrial membrane potential of isolated mitochondria from brain was measured as described in Methods.

State 1: without substrate; Glut/Malate: with substrates of glutamate/malate; Suc+Rot: with substrate of succinate plus rotenone. *: $P< 0.05$. n=3–4.

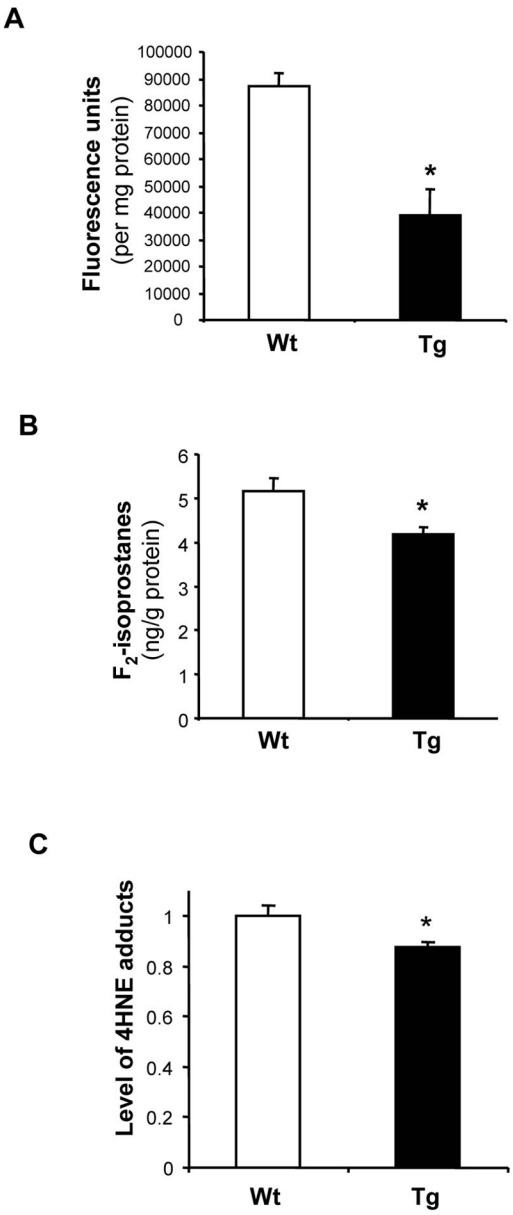

Figure 3. Reduced cellular ROS and oxidative damage in Tg(PRDX3) mice

A. Levels of cellular ROS in skin fibroblasts from Tg(PRDX3) mice and Wt mice were measured by a DCF fluorescence method. The data are presented as mean ± SEM of data obtained from three independent lines. *: P< 0.05. n=5

B. Levels of F_2-isoptostanes in liver tissues of Wt and Tg(PRDX3) were determined as described by Ran et al (2007). The data are expressed as mean ± SEM. *P<0.05. n=5

C. 4-HNE adducts in mitochondria proteins from liver tissues of Tg(PRDX3) mice and Wt mice were determined by Western blots and quantified as described in Methods. The mean value of 4-HNE adducts obtained from Wt mice was artificially assigned as 1, and the relative values are presented as mean ± SEM. *: P<0.05. n= 4–5.

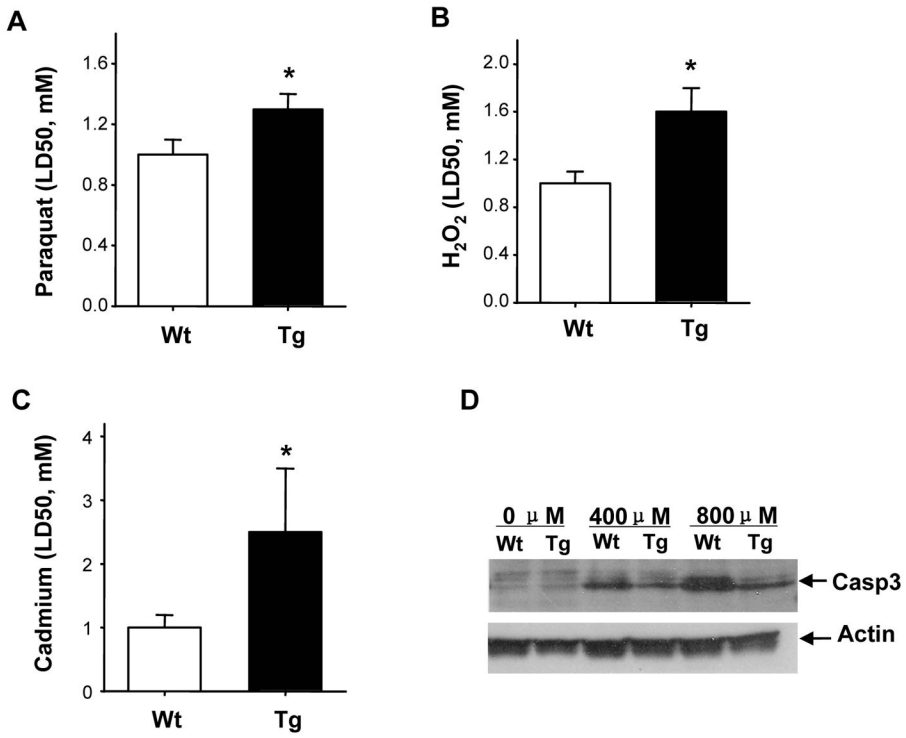

Figure 4. Increased stress resistance of fibroblasts from Tg(PRDX3) mice

Fibroblasts from Tg(PRDX3) and Wt mice were exposed to paraquat (**A**), H_2O_2 (**B**) and cadmium (**C**), and the LD50 (lethal dose, 50%) value for each agents was determined as described by Salmon et al (2005). The data are expressed as mean ± SEM. *: $P<0.05$. n=3–6 **D.** Fibroblasts were treated with t-BOOH for 6 hours, and the level of p20 (a subunit of activated caspase-3) were determined by Western blot.

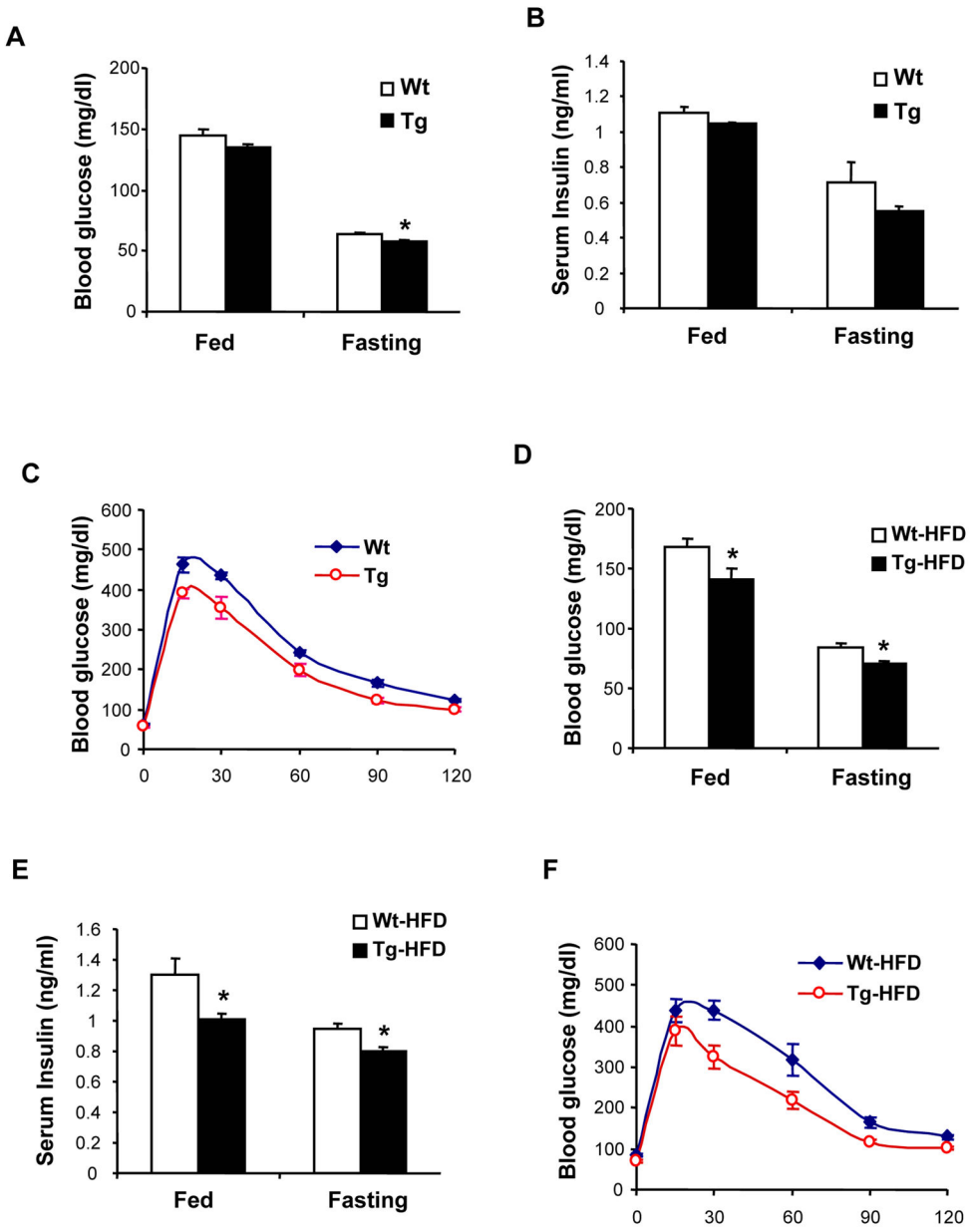

Figure 5. Blood glucose and insulin levels in Tg(PRDX3) mice

A. Blood glucose levels of Tg(PRDX3) and Wt mice of female mice that were 2–3 months of age at fed state and fasting state were determined as described in Methods. The data are presented as mean ± SEM. *: P< 0.05. n=6–7

B. Plasma insulin levels of Tg(PRDX3) and Wt mice at fed state (basal) and fasting state were determined as described in Methods. The data are presented as mean ± SEM. n=6.

C. Glucose tolerance of Tg(PRDX3) and Wt mice. The data are presented as mean ± SEM. n=6–7.

D. Blood glucose levels of Tg(PRDX3) and Wt female mice after feeding a high-fat diet for 8 weeks. The data are presented as mean ± SEM. Wt-HF: HFD fed Wt mice. Tg-HF: HFD-fed Tg(PRDX3) mice. *: P< 0.05. n=8

E. Plasma insulin levels of Tg(PRDX3) and Wt female mice after feeding a high-fat diet for 8 weeks. *: P< 0.05. n=4.

F. Glucose tolerance of Tg(PRDX3) and Wt female mice feeding a high-fat diet for 8 weeks. The data are presented as mean ± SEM. n=8

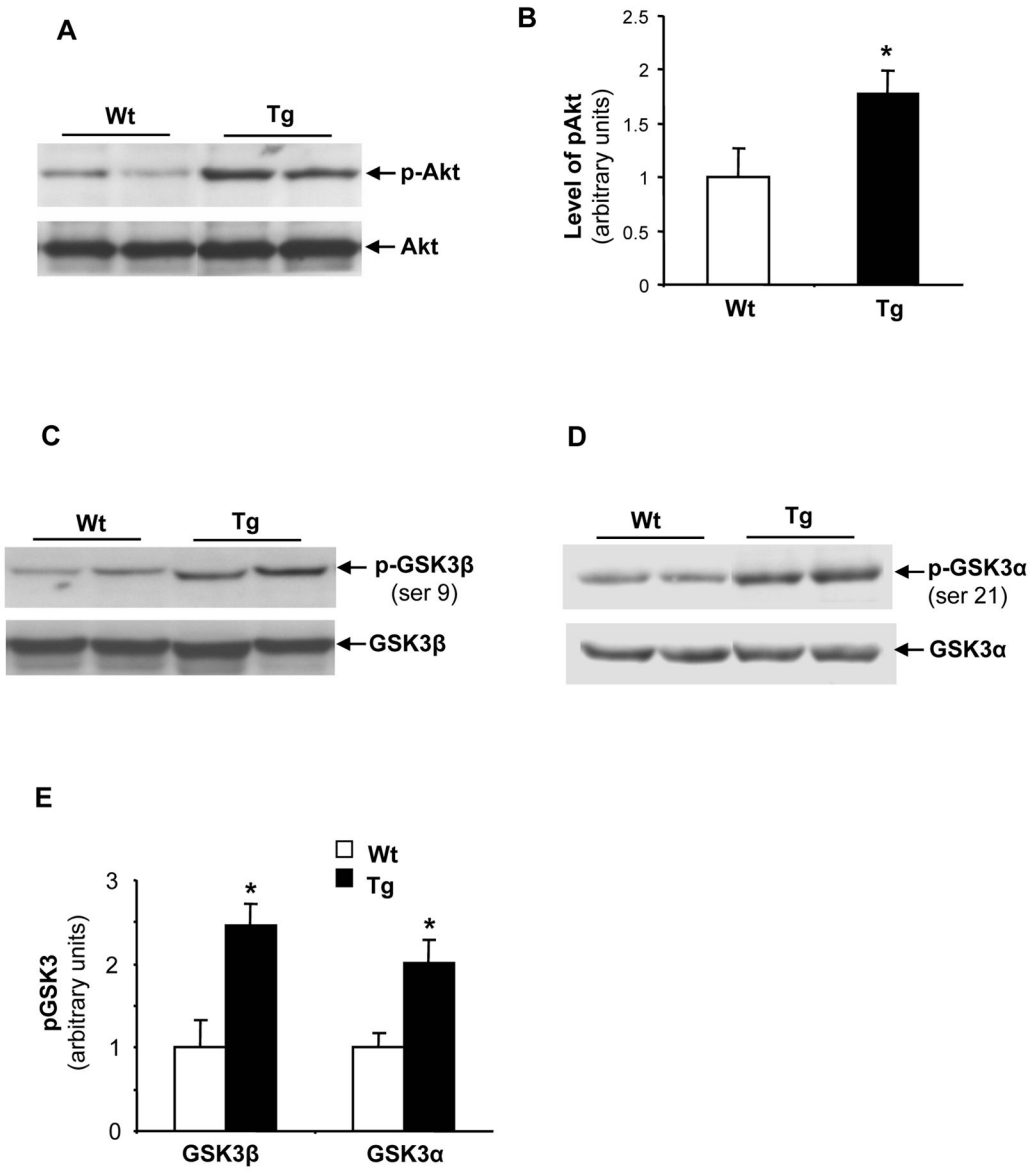

Figure 6. Inhibition of GSK3 in Tg(PRDX3) mice

A. Western blots showing levels of phosphorylated Akt and total Akt protein in liver tissues of Tg(PRDX3) and Wt mice.

B. The quantified results of phosphorylated Akt. The data are presented as mean ± SEM. *P< 0.05. n=6

C. Western blots showing levels of phosphorylated GSK3β (ser9) and total GSK3β protein in liver tissues of Tg(PRDX3) and Wt mice.

D. Western blots showing levels of phosphorylated GSK3α (ser21) and total GSK3α protein in liver tissues of Tg(PRDX3) and Wt mice.

E. The quantified results of phosphorylated GSK3β and GSK3α proteins. The data are presented as mean ± SEM. *P< 0.05. n=6